Journal of Electroceramics, 8, 209–214, 2002

Processing of Piezoelectric Fiber/Polymer Composites with 3-3 Connectivity

B. JADIDIAN,* M. ALLAHVERDI, F. MOHAMMADI & A. SAFARI

Department of Ceramic and Materials Engineering, Rutgers University, 607 Taylor Rd, Piscataway, NJ 08854, New Jersey, USA

Submitted August 28, 2001; Revised August 28, 2001; Accepted March 22, 2002

Abstract. The processing-property relationship of dielectric and piezoelectric properties of 3-3 fabric composites was studied. Fine PZT green fibers were woven into plane fabric, cut in 3×3 cm^2 pieces, and stacked 8 plies high. The stacks were heat-treated with and without applied pressure and then embedded in soft and hard polymers. Increasing the applied pressure increased the density and electromechanical properties of composites due to the improvement of the ply-to-ply sintering. At an optimum uniaxial pressure of 588 Pa, the piezoelectric and dielectric properties of composites with ≈41 vol% PZT and soft matrix were $K = 230$, $d_{33} = 220$ pC/N, $g_{33} = 108$ mV/m, and $d_{33}g_{33} = 23778 \times 10^{-15}$ m^2/N. The porosity-permittivity relationship was used to determine the depolarizing factor of the composites, which represented the degree of ceramic continuity between electrodes. In general, composites with soft matrix had higher electromechanical properties than those with hard matrix. The effect of poling direction on the piezoelectric and dielectric properties was also investigated. The composites poled along the PZT fibers had higher electromechanical properties than those poled perpendicular to the PZT fibers.

Keywords: PZT, piezoelectric, composite, fabric, large area

1. Introduction

Fabrication of large area-fine scale piezoelectric composites can be a significant achievement for applications such as hydrophone, transducers, sensors, actuators, and vibration/noise cancellation. In the past, various methods have been used to build 3-3 composites only in small scale and an area not exceeding a few centimeters. These processes will be reviewed in the following and their main obstacles for the production of large area composites will be described.

In composites with 3-3 connectivity, the ceramic and polymer phases are continuous in three dimensions. The replamine was the first process used to form composite with such connectivity [1]. In this process, a coral skeleton was impregnated with a wax and the calcium carbonate was then leached away to form a porous, burnable structure, which was later refilled with PZT slip. After the wax was burned out and the ceramic was sintered, the porous PZT replica was backfilled with a high purity silicone rubber. The replamine composites exhibited a dielectric constant ≈100 and $d_{33} = 160$ pC/N. Although these composites showed an improvement in hydrostatic piezoelectric properties over solid PZT ceramics, there are two disadvantages associated with replamine process. First, the coral is not abundant and secondly the porosity structure, including the pore size, pore distribution, and their interconnection cannot be controlled.

To overcome these problems, a simple method called BURPS (BURnd-out Plastic Spheres) was developed to fabricate 3-3 piezocomposites with properties similar to the replamine composites [2, 3]. In this method, PZT powder and polymethylmethacrylate (PMMA) spheres were first mixed and pressed to form pellets. Next, the PMMA spheres were volatilized and the pellets were sintered, leaving a porous structure that was backfilled with silicone rubber or stiff epoxy. Several attempts were further made in Japan to improve this technique for mass production of porous PZT ceramics [4–7]. Despite its simplicity, this process could not

*Present address: Layered Manufacturing, Inc., 101A Phelps Avenue, New Brunswick, NJ 08901, New Jersey, USA.

offer any advantages for a better control of the porosity structure.

Other methods such as relic processing [8–13], distorted reticulated ceramics [14, 15], and ladder and/or 3-D honeycomb structures [16, 17] were exploited to fabricate 3-3 composites. In the relic process, a woven carbon template was impregnated with an alkoxide PZT stock solution. The heat-treatment was then carried out to remove the carbon and transform the metal ions into a PZT relic with a replica of the original carbon material. The PZT replica was then sintered and embedded in a thermally curable polymer. Although large area composites can be made with this method, the major disadvantage of the relic process is the toxicity of alkoxide solutions.

Reticulated composites were formed by coating organic foam substrates (i.e. polyurethane) with PZT ceramic slurry. The coated foam was pyrolized and sintered to form a structure composed of hollow ceramic ligaments which was then filled with polymer. The first ladder structure was formed by arranging ceramic bars in a network type. After sintering, the structure was embedded in silicone rubber. The ladder composites had a piezoelectric voltage coefficient four times larger than that of conventional PZT ceramics. In addition, rapid prototyping techniques of fused deposition modeling (FDM) and fused deposition of ceramics (FDC) were used to make ladder and 3-D honeycomb composites. In the FDM technique, a 3-D plastic mold was prepared and filled with PZT slurry. While in the FDC process, a mixture of PZT and polymer was directly deposited in the form of a three-dimensional ladder structure. Either structure was then heat treated to burn the organic, sintered, and filled with epoxy.

In this work, the green continuous PZT-5H (Morgan Matroc Inc., Cleveland, OH) fibers produced by the Viscous Suspension Spinning Process (VSSP) at Advanced Cerametrics Inc. (ACI) [18–20] were woven to form a large area plane fabric. The green PZT fibers had diameters typically ranging from 25 to 70 μm. The objectives of this work were:

1. To demonstrate the feasibility of forming large area PZT fabrics and to build fine scale piezoelectric fiber/polymer composites.
2. To study the effect of processing on the dielectric and piezoelectric properties of such composites. This included applied pressure, type of polymer matrix, and poling direction.

2. Experimental Methods and Procedures

Plane PZT fabrics (30 cm × 200 cm) were woven using a bundle of 5000 fibers as picks and 800 fibers as ends, as shown in Fig. 1. The plain weave fabric was cut into 3 × 3 cm^2 sheets which were stacked 8 plies high. The samples were placed on platinum foils sitting in an alumina crucible. The organic removal was performed at 550°C for 4 hours with a 1.5°C/min ramp to make sure that all organic had burned off. Then, samples were bisque-fired at 780°C for 1 hour with a 3.5°C/min ramp to strengthen them for handling, followed by sintering at 1285°C in a lead controlled atmosphere. The organic burnout and sintering were performed with and without uniaxial pressure on the samples. The pressure was applied by placing a weight, in the form of platinum foil and alumina plates on top of the samples. Weights corresponding to pressures of 0, 294, 392, 490, 588, 686 and 882 Pa were applied to the samples.

To fabricate composites, the sintered PZT stacks were embedded in two different types of epoxy. The Spurr (Ernest F Fullam, Inc., Latham, NY) and Eccogel-65 (Emerson and Cumming, Deway and Almy Chemical Division, Canton, MA) were used as hard and soft matrices, respectively. The composites were sliced into 2 mm thick samples, polished to 1.5 mm thickness, and dried at 70°C for 4 hours to remove the moisture that was absorbed during the polishing step. Electrodes were then applied using air-dried silver paint (No. 200, Demetron, Liepziger, Germany). Composites were poled via the Corona method [21] at 28 kV for 20 minutes while temperature decreased from 60 to 45°C.

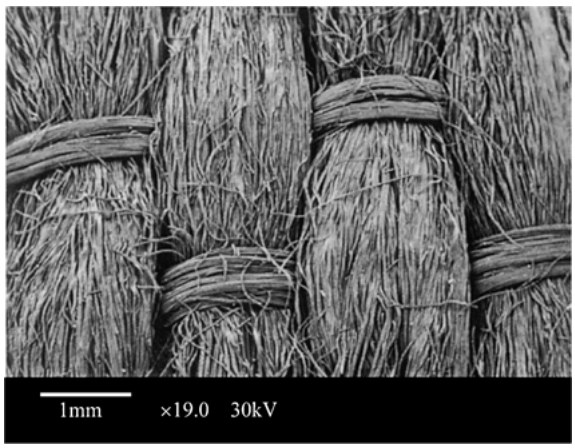

Fig. 1. SEM picture of a plane PZT fabric containing 5000 fibers as picks and 800 fibers as ends.

The microstructure of sintered stacks was examined using electron microscopy (Model 1200 SEM, Amray Corporation, Bedford, MA). Capacitance, C_p, and dissipation factor, $\tan\delta$, were measured at 1 KHz using an RLC Digibridge (1689M precision, GenRad Inc., Bolton, MA). The piezoelectric charge coefficient, d_{33}, of the composites was determined at 100 Hz using a Berlincourt Piezo Meter (CPDT-3300-Chanel Product, Inc., Cleveland, OH) with two flat probes.

3. Results and Discussion

3.1. *Effect of Pressure on the Electromechanical Properties*

Table 1 summarizes the physical and electromechanical properties of the composites embedded in Eccogel-65 epoxy. The composites were poled through their thickness with the electric potential being perpendicular to the fabric plies. When no pressure was applied on the stacks, the composites showed the lowest electromechanical properties because the fabric plies did not sinter strongly to each other. The composite had a 2(3-3)-2 connectivity since the plies were almost discrete and separated by layers of polymer. Thus, the composites represented a 2-2 connectivity instead of a 3-3 pattern. However, due to the existence of polymer between the individual fibers in each ply, every layer of fabric was considered to be a 3-3 composite. Figure 2 is a close-up of Fig. 1 that shows individual PZT fibers within a ply. The poor cross sintering between plies as well as the individual fibers within plies gave rise to the discontinuity of ceramic phase between either electrode. Therefore, the ceramic phase was not efficiently poled and the lowest electromechanical properties were observed.

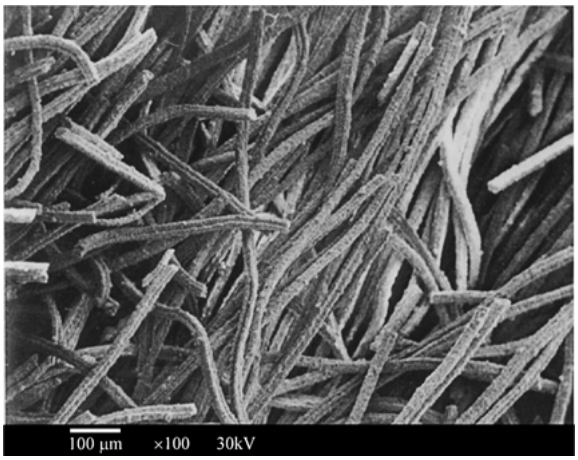

Fig. 2. A close-up of the Fig. 1 displaying individual PZT fibers within a sheet.

The application of uniaxial pressure during organic burnout and sintering improved the cross sintering between plies and thereby enhanced the physical, piezoelectric, and dielectric properties of the composites. Figure 3 displays variation of the density of composites with the applied pressure. Below ≈400 Pa, the application of pressure rapidly improved the density of composites and significantly enhanced the cross sintering between the plies. Further increase in pressure slightly changed the density of the composites by improving the cross sintering between the individual PZT filaments within each ply. This explains the linear increase in dielectric constant with pressure that is shown in Fig. 4.

The improvement of cross sintering was verified using the porosity-dielectric constant relationship introduced by Okazaki and Igarashi [22]. From dielectric point of view, a 3-3 composite was considered as a uniformly continuous dielectric medium including porosity filled with epoxy, which hereafter is referred to

Table 1. The physical and electromechanical properties of composites embedded in Eccogel-65 epoxy.

Pressure (Pa)	Density (g/cm^3)	PZT (vol%)	Polymer (vol%)	d_{33} (pC/N)	K	$\tan\delta$	g_{33} (10^{-3} V m/N)	$d_{33}g_{33}$ (10^{-15} m^2/N)	N_i ($\times10^{-6}$)
0	2.90	26.50	73.50	70	100	0.03	79	5537	25
294	3.40	35.80	66.20	100	140	0.04	81	8071	16
392	3.60	36.80	63.20	160	170	0.04	106	17016	12
490	3.65	37.50	62.50	190	190	0.03	113	21469	9
588	3.68	37.90	62.10	220	230	0.03	108	23778	6
686	3.70	38.20	61.80	220	250	0.04	99	21876	5
882	3.75	39.00	61.00	220	280	0.03	89	19532	4

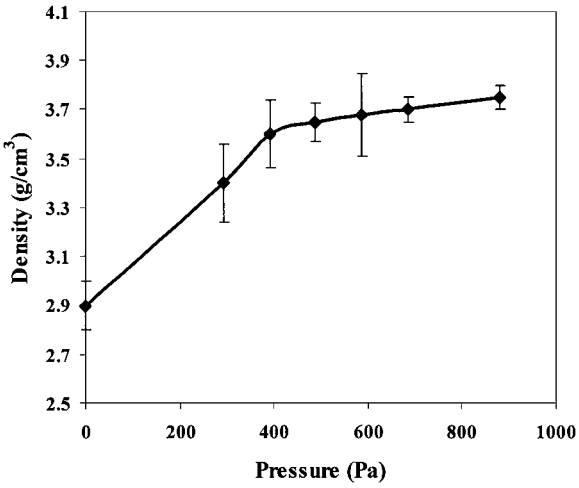

Fig. 3. The plot of density of composites with Eccogel-65 matrix versus applied pressure.

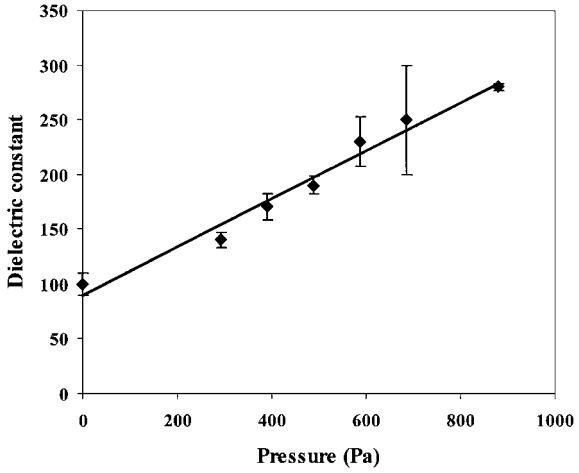

Fig. 4. Plot of dielectric constant of composites with Eccogel-65 matrix versus applied pressure.

polymer volume fraction. The composite depolarizing factor was calculated using:

$$K_{\text{app}} - 1 = \frac{\left[\left(1 - \frac{P}{100}\right)(K_{\text{st}} - 1)\right]}{[1 + N_i(KK_{\text{st}} - 1)]}$$

where K_{app}, K_{st}, are the apparent dielectric constant of a ceramic dielectric with and without pores, respectively, and P and N_i are the polymer volume fraction and depolarizing factor, respectively. Table 1 represents the depolarizing factor of composites by considering $K_{\text{st}} \approx 4800$ for bulk PZT-5H and $P = (100-\text{PZT vol\%})$.

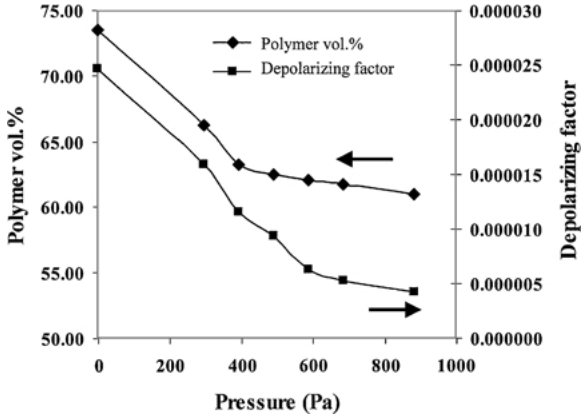

Fig. 5. The plot of porosity volume fraction and depolarizing factor versus applied pressure for composites with Eccogel-65 matrix.

Figure 5 shows the variation of porosity volume fraction and depolarizing factor, N_i, versus applied pressure. In the absence of applied pressure, composites had the highest polymer volume fraction and depolarizing factor. While the application of pressure on the stacks remarkably reduced the polymer content and depolarizing factor below 400 and 588 Pa pressure, respectively. However, further increase of pressure slightly changed the polymer vol% and depolarizing factor. In a fully interconnected dielectric such as a honeycomb structure, the depolarizing factor approaches zero [6]. Therefore, in a composite with a good connectivity, the depolarizing factor is small and any minute change in polymer vol% and N_i will have a prominent effect on increase and/or decrease of dielectric constant. This also explains the increase of dielectric constant with pressure above 588 Pa in Fig. 4.

The plot of piezoelectric charge coefficient versus applied pressure is shown in Fig. 6. The d_{33} value increased with pressure and saturated at 588 Pa, which agrees with slight variation of composite density above this pressure. Figure 7 represents the variation of piezoelectric voltage coefficient versus applied pressure. The g_{33} value reached a maximum at 490 Pa and then decreased with further increase in pressure. The piezoelectric figure of merit, $d_{33}g_{33}$, showed a similar trend with applied pressure, as shown in Fig. 7.

3.2. *Effect of Polymer Matrix on the Electromechanical Properties of Composites*

The effect of polymer matrix with different stiffness was examined on the electromechanical properties

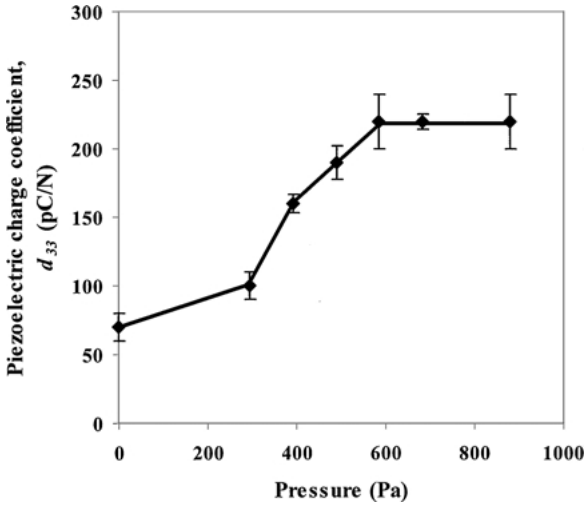

Fig. 6. The plot of piezoelectric charge coefficient of composites with Eccogel-65 matrix versus the applied pressure.

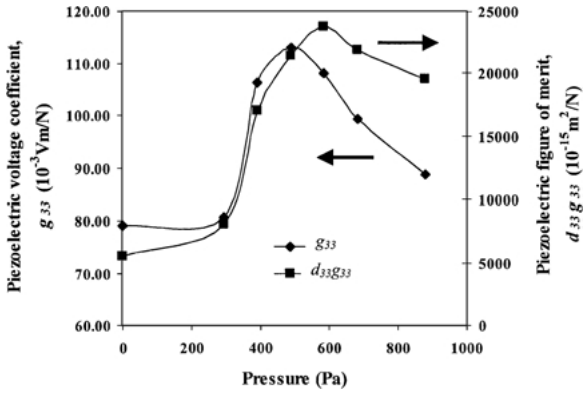

Fig. 7. The plot of piezoelectric voltage coefficient for composites with Eccogel-65 matrix versus applied pressure.

of fabric composites. Sintered stacks were embedded in hard Spurr epoxy, cured, polished, and poled in the same manner as the soft Eccogel samples. Table 2 compares the electromechanical properties of composites embedded in two different polymers. The ($\perp$) sign denotes that the electric potential during poling was perpendicular to the fabric plies. The variation of physical and electromechanical properties of Spurr composites with applied pressure had similar trend to the Eccogel samples. However, Spurr composites had considerably lower electromechanical properties than Eccogel composites. At 588 Pa pressure, the dissipation factor, $\tan\delta$, and dielectric constant of the Spurr composites were two times smaller than those of Eccogel composites. This was expected because pure Eccogel-65 has almost one order of magnitude higher electrical resistance than pure Spurr epoxy. Therefore this allowed a higher E-field to pass through the ceramic phase in Eccogel composites leading to a more efficiently poled samples.

In addition to the efficacy of poling process, the Eccogel-65 like many other soft epoxies also offered a high mechanical compliance and a better stress transfer to the ceramic phase in the composites. As a result, the Eccogel samples could develop higher polarization and consequently $\approx$3 times higher d_{33} values. The higher electrical loss in Eccogel samples corresponded to the higher electrical loss of pure Eccogel-65. The dielectric loss values for pure Eccogel and Spurr epoxy measured at 1 KHz were 0.089 and 0.026, respectively.

3.3. *Effect of Poling Direction on the Electromechanical Properties of Composites*

Both flexible and stiff composites were also poled with the electric field applied parallel to their fabric plies, as indicated by ($\parallel$) sign. Table 2 compares the electromechanical properties of samples poled in two different directions. At a similar ceramic volume fraction, the dielectric constant of the "parallel" poled composites

Table 2. The electromechanical properties of composites embedded in two different polymer matrices and poled under different electrical potential directions.

Sample ID	PZT (vol%)	Polymer (vol%)	d_{33} (pC/N)	K	$\tan\delta$	g_{33} (10^{-3} Vm/N)	$d_{33}g_{33}$ (10^{-15} m^2/N)	N_i ($\times10^{-6}$)
Spurr-294 (Pa) $\perp$ E-field	33.00	67.00	60	90	0.02	75	4500	39
Spurr-588 (Pa) $\perp$ E-field	37.00	63.00	80	130	0.02	69	5520	20
Spurr-588 (Pa) $\parallel$ E-field	37.50	62.50	120	290	0.02	47	5640	4
Eccogel-588 (Pa) $\perp$ E-field	37.90	62.10	220	230	0.03	108	23778	6
Eccogel-588 (Pa) $\parallel$ E-field	38.00	62.00	250	490	0.04	58	14500	2

increased by a factor of two. This was attributed to a better continuity of ceramic phase between electrodes in the samples, which was verified by comparing the depolarizing factors of "perpendicular" and "parallel" poled composites. The depolarizing factors of "parallel" poled Spurr and Eccogel composites are approximately 5 and 3 times, respectively, smaller than those of the corresponding "perpendicular" poled composites.

4. Summary

The processing of 3-3 composites was studied using woven PZT fibers. The PZT fabric was cut in square pieces and stacked 8 plies high. The organic content was removed and samples were sintering with and without applied pressure during heat treatment. The effect of poling direction and type of polymer matrix on the dielectric and piezoelectric properties of composites were studied. The experiments showed that:

1. In the absence of applied pressure, composites had the lowest dielectric and piezoelectric properties when embedded in both soft and hard polymer. A better cross sintering between the plies was developed by applying pressure on the samples during heat treatment steps. The piezoelectric charge coefficient of composites remarkably improved with increasing applied pressure and saturated at 588 Pa. However, the dielectric properties of composites increased linearly even above this pressure.
2. The type of polymer matrix had a considerable effect on the electromechanical properties of the composites. In comparison, composites with hard matrix had lower dielectric and piezoelectric properties than composites with soft matrix.
3. The composites poled along PZT fibers ("parallel" poled) had higher electromechanical properties than "perpendicular" poled composites.

Acknowledgments

The authors would like to acknowledge Advanced Cerametrics Inc. for supplying the PZT green fibers under STTR contract for ONR, and financial support of the Office of Naval Research under contract number N00014-94-1-0585 which made this work possible.

References

1. D.P. Skinner, R.E. Newnham, and L.E. Cross, *Mat. Res. Bull.*, **13**, 599 (1978).
2. T.R. Shrout, W.A. Schulze, and J.V. Biggers, *Mat. Res. Bull.*, **14**, 1553 (1979).
3. K. Rittenmyer, T. Shrout, W.A. Schulze, and R.E. Newnham, *Ferroelectrics*, **41**, 189 (1982).
4. K. Hikita, K. Yamada, and M. Nishioka, *Jap. J. Appl. Phys.*, **22**, Supplement 22-2, 64 (1983).
5. K. Hikata, K. Yamada, M. Nishioka, and M. Ono, *Ferroelectrics*, **49**, 265 (1983).
6. T. Hayashi, S. Sugihara, and K. Okazaki, *Jap. J. Appl. Phys.*, **30**(9B), 2243 (1991).
7. K. Nagata, H. Igarashi, K. Okazaki, and R.C. Bradt, *Jap. J. Appl. Phys.*, **19**(1), 37 (1980).
8. R.J. Card, M.P. O'Toole, and A. Safari, U.S. Pat. No. 4726099, February 23 (1988).
9. R.J. Card, M.P. O'Toole, and A. Safari, U.S. Pat. No. 4933230, June 12 (1990).
10. D.J. Waller and A. Safari, *J. Am. Ceram. Soc.*, **75**(6), 1648 (1992).
11. D.J. Waller, A. Safari, and R.J. Card, *J. Am. Ceram. Soc.*, **73**(11), 3503 (1990).
12. S.S. Livneh, S.M. Ting, and A. Safari, *Ferroelectrics*, **157**, 421 (1994).
13. S.M. Ting, V.F. Janas, and A. Safari, *J. Am. Ceram. Soc.*, **79**(6), 1689 (1996).
14. M.J. Creedon and W.A. Schulze, *Ferroelectrics*, **153**, 333 (1994).
15. M.J. Creedon, S. Gopalakrishnan, and W.A. Schulze, in *Proceedings of the 9th International Symposium on the Application of Ferroelectrics* (Institute of Electrical and Electronic Engineers, Piscataway, NJ 1995), p. 299.
16. M. Miyashita, K. Takano, and T. Tado, *Ferroelectrics*, **28**, 397 (1980).
17. A. Bandyopahayay, R.K. Panda, V.F. Janas, M.K. Agrawala, S.C. Danforth, and A. Safari, *J. Am. Ceram. Soc.*, **80**(6), 1366 (1997).
18. R.B. Cass, *Am. Cerm. Soc. Bul.*, **70**(3), 424 (1991).
19. J.D. French and R.B. Cass, *Am. Ceram. Soc. Bull.*, **77**(5), 61 (1998).
20. J.D. French, G.E. Weitz, J.E. Luke, R.B. Cass, B. Jadidian, P. Bhargava, and A. Safari, in *Proceedings of SPIE—The International Society for Optical Engineering*, vol. 3044 (Society of Photo-Optical Instrumentation Engineers, Bellingham, WA 1997), p. 406.
21. D. Waller and A. Safari, *Ferroelectrics*, **87**, 189 (1990).
22. K. Okazaki and H. Igarashi, in *Proc. Int. IEEE Symp. of Applications of Ferroelectrics*, Minneapolis, June 13–15 (Institute of Electrical and Electronic Engineers, Piscataway, NJ 1979).